Paper 22

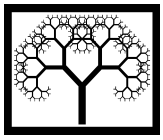

Proceedings of the Eleventh International Conference on Computational Structures Technology,
B.H.V. Topping, (Editor),
Civil-Comp Press, Stirlingshire, Scotland

Computer-Based Nonlinear Analysis for the Seismic Performance Assessment of Three-Dimensional Steel Frameworks

C.G. Chiorean, G. Tarta, I. Marchis and M. Buru
Faculty of Civil Engineering
Technical University of Cluj-Napoca, Romania

Abstract

This paper presents an integrated system for advanced structural analysis and seismic performance evaluation of three-dimensional steel frameworks with rigid or flexible connections. The non-linear inelastic static analysis employed uses the accuracy of the fibre-finite element approach for inelastic frame analysis and addresses its efficiency and modelling shortcomings through the use of only one element to model each physical member of the frame. The proposed model has been implemented in a matrix structural-analysis computer program that also accounts for geometric nonlinearity and semi-rigid connections. The proposed software is presented as an efficient, reliable tool ready to be implemented into design practice for advanced analysis and pushover analysis of spatial frame structures.

Keywords: plastic zone analysis, semi-rigid space frameworks, large deflections, advanced analysis, pushover analysis.

1 Introduction

With the rapid advancement of computer technology, research works are currently in full swing to develop advanced nonlinear inelastic analysis methods and integrate them into the new and more rational advanced analysis and design procedures [1-5]. Reliable nonlinear analysis tools are, for instance, essential in performance-based earthquake engineering, and advanced analysis methodologies, that involves accurate predictions of inelastic limit states up or beyond to structural collapse. The need for accurate yet computational efficient tools for the nonlinear inelastic analysis of real large-scale 3D steel frameworks forms the main motivation behind of this work. Essentially, nonlinear inelastic analysis employed herein uses the accuracy of the fiber elements approach for inelastic frame analysis and address its efficiency and modelling shortcomings both to element level, through the use of

only one element to model each physical member of the frame, and to cross-sectional level through the use of path integral approach to numerical integration of the cross-sectional nonlinear characteristics. The computer program developed here fully integrates a 3D eigen analysis and a 3D non-linear inelastic analysis, based on fiber member model, in conjunction with advanced performance evaluation functions, following an approach outlined in the next sections.

2 Formulation of the proposed analysis method

The following assumptions are adopted in the formulation of analytical model: (1) plane section remain plane after flexural deformation; warping and cross-section distortion are not considered; (2) torsional buckling do not occur; (3) small strain but arbitrarily large displacements and rotations are considered; (4) the connection element is of zero length. The proposed approach is based on the most refined type of second order inelastic analysis, *distributed plasticity model*, where elasto-plastic behaviour is modelled accounting for spread-of plasticity effect in sections and along the element and employs modelling of structures with only one line element per member, which reduces the number of degree of freedom involved and the computational time. The above assumptions allow the formulation details to be considered on two distinct levels, namely, the cross-sectional level and the member longitudinal axis level. Thus the nonlinear response of a beam-column element can be computed as a weighted sum of the response of a discrete number of cross-sections (i.e. stations) that are located at the numerical integration scheme points.

2.1 Cross-section analysis

The cross-section stiffness may be modelled by explicit integration of stresses and strains over the cross-section area (e.g., as *micro model formulation*) or through calibrated parametric equations that represent force-generalized strain curvature response (e.g. *macro model formulation*).

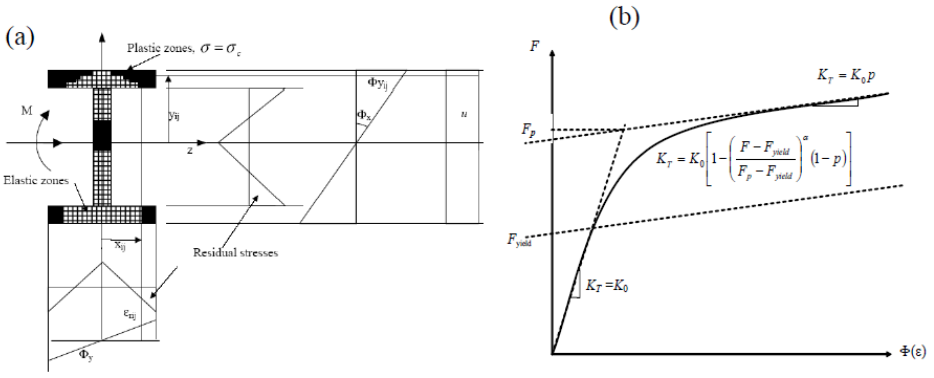

Figure 1: (a) Micro model formulation: fiber cross-section analysis; (b) Macro model formulation: proposed force-strain relationships.

2.1.1 Micro model formulation

Gradual plastification through the cross-section subjected to combined action of axial force and bi-axial bending moments is described through basic equilibrium, compatibility and material nonlinear constitutive equations. In this way, the states of strain, stress and yield stress are monitored explicitly during each step of the analysis, the arbitrary cross-sectional shape and the effect of material imperfections such as residual stresses are accurately included in the analysis. Inverse Ramberg-Osgood stress-strain relationships both in tension and in compression are assumed (Eq.1):

$$\sigma(\varepsilon) = \sigma_y \left[1 + \left(\frac{|\varepsilon|}{\varepsilon_y} \right)^n \right]^{-\frac{1}{n}} \frac{\varepsilon}{\varepsilon_y} \tag{1}$$

where σ_y and ε_y represents the yield stress and yield strain respectively. In this way, via shape parameter (n) either elastic-perfect plastic or gradual yielding may be included in the analysis. The magnitude and distribution of residual stresses in hot-rolled members depend on the type of cross section and manufacturing processes and different patterns are proposed. In the US, the residual stress is considered constant in the web although, when the depth of a wide flange section is large, it varies more or less parabolically. Another possible residual stress pattern in the web is the one simplified by a linear variation as used in European calibration frames (Fig.1a).

2.1.1.1 Elasto-plastic flexural rigidity of cross-section

Considering the cross-section subjected to the action of the external bending moments (M_{x0}, M_{y0}) about each global axes and axial force (N_0) as shown in Figure 1a. Under the above assumptions the resultant strain distribution corresponding to the curvatures about global axes $\mathbf{\Phi} = \begin{bmatrix} \Phi_x & \Phi_y \end{bmatrix}$ and the axial strain u can be expressed in point $\mathbf{r} = \begin{bmatrix} x & y \end{bmatrix}$ in a linear form as:

$$\varepsilon = u + \Phi_x y + \Phi_y z + \varepsilon_0 = u + \mathbf{\Phi r}^T + \varepsilon_0 \tag{2}$$

where ε_0 is the initial deformation produced by residual stresses. The equilibrium is satisfied when the external forces (N_0, M_{x0}, M_{y0}) are equal to the internal ones. These conditions can be represented mathematically in terms of the following nonlinear system of equations as:

$$\begin{cases} \int_{A_s} \sigma\left(\varepsilon\left(u, \phi_x, \phi_y\right)\right) dA_s - N_0 = 0 \\ \int_{A_s} \sigma\left(\varepsilon\left(u, \phi_x, \phi_y\right)\right) y dA_s - M_{x0} = 0 \\ \int_{A_s} \sigma\left(\varepsilon\left(u, \phi_x, \phi_y\right)\right) x dA_s - M_{y0} = 0 \end{cases} \tag{3}$$

in which u, ϕ_x, ϕ_y represent the unknowns. The above system can be solved numerically using, for instance, the load-controlled Newton method and taking into

account the fact that the stresses are implicit functions of the axial strain and curvatures through the resultant strain distribution given by the Eq. (2). In this way, for given bending moments and axial force we can obtain the strain distribution and the location and inclination of the neutral axis. This system can be rewritten in terms of non-linear system of equations in the following general form:

$$\mathbf{F}(\mathbf{X}) = \mathbf{f}^{\text{int}} - \mathbf{f}^{ext} = \mathbf{0} \tag{4}$$

where $\mathbf{X} = \begin{bmatrix} \varepsilon_0 & \phi_x & \phi_y \end{bmatrix}^T$, the external and internal loading vectors can then be represented by:

$$\mathbf{f}^{ext} = \begin{bmatrix} N_0 \\ M_{x0} \\ M_{y0} \end{bmatrix}$$

$$\mathbf{f}^{int} = \begin{bmatrix} N_{\text{int}} = \int_{A_s} \sigma\left(\varepsilon\left(u, \phi_x, \phi_y\right)\right) dA_s \\ M_x^{int} = \int_{A_s} \sigma\left(\varepsilon\left(u, \phi_x, \phi_y\right)\right) y dA_{cs} \\ M_y^{int} = \int_{A_s} \sigma\left(\varepsilon\left(u, \phi_x, \phi_y\right)\right) x dA_s \end{bmatrix} \tag{5}$$

The Eqns. (4) are solved numerically using the Newton-Raphson method, and results in three recurrence relationships to obtain the unknowns u and $\mathbf{\Phi}$ and then flexural EI and axial EA rigidity modulus can be computed. According to the Newton iterative method, the iterative changes of unknowns vector $\mathbf{X}$ can be written as:

$$\mathbf{X}^{k+1} = \mathbf{X}^k - \mathbf{F}'\left(\mathbf{X}^k\right)^{-1} \mathbf{F}\left(\mathbf{X}^k\right), k \geq 0 \tag{6}$$

where **F'** represents the Jacobian (or tangent cross-section stiffness matrix) of the nonlinear system (4) and can be expressed as:

$$\mathbf{F}' = \left(\frac{\partial \mathbf{F}}{\partial \mathbf{X}}\right) = \begin{bmatrix} \frac{\partial N^{\text{int}}}{\partial u} & \frac{\partial N^{\text{int}}}{\partial \phi_x} & \frac{\partial N^{\text{int}}}{\partial \phi_y} \\ \frac{\partial M_x^{\text{int}}}{\partial u} & \frac{\partial M_x^{\text{int}}}{\partial \phi_x} & \frac{\partial M_x^{\text{int}}}{\partial \phi_y} \\ \frac{\partial M_y^{\text{int}}}{\partial u} & \frac{\partial M_y^{\text{int}}}{\partial \phi_x} & \frac{\partial M_y^{\text{int}}}{\partial \phi_y} \end{bmatrix} \tag{7}$$

Explicitly the expressions of the Jacobian's coefficients are given in Eqs. 8.

$$
\begin{aligned}
k_{11} &= \frac{\partial N^{int}}{\partial u} = \frac{\partial}{\partial u}\left[\int_{A_{cs}} \sigma\left(\varepsilon\left(u,\phi_x,\phi_y\right)\right)dA_s\right] = \int_{A_s} \frac{\partial \sigma}{\partial \varepsilon}\frac{\partial \varepsilon}{\partial u} dA_s = \int_{A_s} E_T dA_s \\
k_{12} &= \frac{\partial N^{int}}{\partial \phi_x} = \frac{\partial}{\partial \phi_x}\left[\int_{A} \sigma\left(\varepsilon\left(u,\phi_x,\phi_y\right)\right)dA\right] = \int_{A_s} \frac{\partial \sigma}{\partial \varepsilon}\frac{\partial \varepsilon}{\partial \phi_x} dA_{cs} = \int_{A_s} E_T y dA_s \\
k_{13} &= \frac{\partial N^{int}}{\partial \phi_y} = \frac{\partial}{\partial \phi_y}\left[\int_{A} \sigma\left(\varepsilon\left(u,\phi_x,\phi_y\right)\right)dA\right] = \int_{A_s} \frac{\partial \sigma}{\partial \varepsilon}\frac{\partial \varepsilon}{\partial \phi_y} dA_s = \int_{A_{cs}} E_T x dA_{cs} \\
k_{21} &= \frac{\partial M_x^{int}}{\partial u} = \frac{\partial}{\partial u}\left[\int_{A_s} \sigma\left(\varepsilon\left(u,\phi_x,\phi_y\right)\right)y dA_s\right] = \int_{A_s} \frac{\partial \sigma}{\partial \varepsilon}\frac{\partial \varepsilon}{\partial u} y dA_s = \int_{A_s} E_T y dA_s \\
k_{22} &= \frac{\partial M_x^{int}}{\partial \phi_x} = \frac{\partial}{\partial \phi_x}\left[\int_{A} \sigma\left(\varepsilon\left(u,\phi_x,\phi_y\right)\right)y dA\right] = \int_{A_s} \frac{\partial \sigma}{\partial \varepsilon}\frac{\partial \varepsilon}{\partial \phi_x} y dA_s = \int_{A_s} E_T y^2 dA_s \\
k_{23} &= \frac{\partial M_x^{int}}{\partial \phi_y} = \frac{\partial}{\partial \phi_y}\left[\int_{A} \sigma\left(\varepsilon\left(u,\phi_x,\phi_y\right)\right)y dA\right] = \int_{A_s} \frac{\partial \sigma}{\partial \varepsilon}\frac{\partial \varepsilon}{\partial \phi_y} y dA_{cs} = \int_{A_s} E_T xy dA_s \\
k_{31} &= \frac{\partial M_y^{int}}{\partial u} = \frac{\partial}{\partial u}\left[\int_{A_s} \sigma\left(\varepsilon\left(u,\phi_x,\phi_y\right)\right)x dA_s\right] = \int_{A_s} \frac{\partial \sigma}{\partial \varepsilon}\frac{\partial \varepsilon}{\partial u} x dA_{cs} = \int_{A_s} E_T x dA_s \\
k_{32} &= \frac{\partial M_x^{int}}{\partial \phi_x} = \frac{\partial}{\partial \phi_x}\left[\int_{A} \sigma\left(\varepsilon\left(u,\phi_x,\phi_y\right)\right)x dA\right] = \int_{A_s} \frac{\partial \sigma}{\partial \varepsilon}\frac{\partial \varepsilon}{\partial \phi_x} x dA_{cs} = \int_{A_s} E_T xy dA_s \\
k_{33} &= \frac{\partial M_x^{int}}{\partial \phi_y} = \frac{\partial}{\partial \phi_y}\left[\int_{A} \sigma\left(\varepsilon\left(u,\phi_x,\phi_y\right)\right)x dA\right] = \int_{A_s} \frac{\partial \sigma}{\partial \varepsilon}\frac{\partial \varepsilon}{\partial \phi_y} x dA_{cs} = \int_{A_s} E_T x^2 dA_s
\end{aligned}
\tag{8}
$$

These coefficients are expressed in terms of the tangent modulus of elasticity E_t=dσ/dε. The convergence criterion is expressed as a ratio of the norm of the out-of-balance force vector to the norm of the total applied load. So the solution is assumed to have converged if:

$$
\frac{\sqrt{\mathbf{F}^T\mathbf{F}}}{\sqrt{\mathbf{f}^{ext T}\mathbf{f}^{ext}}} \le TOL \tag{9}
$$

where *TOL* is the specified computational tolerance, usually taken as 1*E*-5. Based on Green's integration formula according to which the domain integrals appearing in the evaluation of internal resultant efforts and tangent stiffness matrix coefficients of the section can be evaluated in terms of boundary integral. This approach is extremely rapid because stress integrals need only be evaluated at a small number of points on the section boundary and rapid convergence is assured by the inclusion of exactly determined tangent stiffnesses and, of great importance, it is assure convergence for any load case. Tangent flexural rigidities for major and minor axis bending under conditions of constant axial load are evaluated by inverting the cross-section tangent stiffness matrix, imposing the condition of constant axial load to obtain a flexural flexibility matrix and inverting this to find the tangent flexural rigidities, about each principal axis, at constant axial load:

$$EI_{tx} = \frac{k_{11}k_{22}k_{33} - k_{11}k_{23}^2 - k_{33}k_{12}^2 + 2k_{12}k_{13}k_{23} - k_{22}k_{13}^2}{k_{11}k_{33} - k_{13}^2}$$
$$EI_{ty} = \frac{k_{11}k_{22}k_{33} - k_{11}k_{23}^2 - k_{33}k_{12}^2 + 2k_{12}k_{13}k_{23} - k_{22}k_{13}^2}{k_{11}k_{22} - k_{12}^2} \quad (10)$$

where stiffness coefficients k_{ij} are given in Eqs. (8). The tangent axial rigidity is computed as $EA_t = \int_{A_s} E_T dA_s$.

2.1.1.2 Determination of the plastic interaction diagrams

A particularly important feature of the present method is represented by the capacity to determine directly the ultimate axial force and bending moments in order to check that they fulfil the ultimate limit state condition. The cross-section subjected to bi-axial bending moments and axial force, reaches its failure limit state when the strain in the extreme steel fiber, attains the ultimate value. Consequently, at ultimate strength capacity the equilibrium is satisfied when the external forces are equal to the internal ones and in the most compressed or tensioned point the ultimate strain is attained. These conditions can be represented mathematically in terms of the following nonlinear system of equations as:

$$\begin{cases} \int_{A_s} \sigma\left(\varepsilon\left(u,\phi_x,\phi_y\right)\right)dA_s - N = 0 \\ \int_{A_s} \sigma\left(\varepsilon\left(u,\phi_x,\phi_y\right)\right)ydA_s - M_x = 0 \\ \int_{A_s} \sigma\left(\varepsilon\left(u,\phi_x,\phi_y\right)\right)xdA_s u - M_y = 0 \\ u + \phi_x y_c\left(\phi_x,\phi_y\right) + \phi_y x_c\left(\phi_x,\phi_y\right) - \varepsilon_u = 0 \end{cases} \quad (11)$$

in which N, M_x, M_y, u, ϕ_x, ϕ_y represent the unknowns, the surface integral is extended over steel area (A_s). In Eqs. (11) the first three relations represent the basic equations of equilibrium for the axial load N and the biaxial bending moments M_x, M_y respectively, given in terms of the stress resultants. The last equation represents the ultimate strength capacity condition in which $x_c\left(\phi_x,\phi_y\right)$ and $y_c\left(\phi_x,\phi_y\right)$ represent the coordinates of the point in which this condition is imposed. The coordinates of the "constrained" point can be always determined for each inclination of the neutral axis defined by the parameters ϕ_x and ϕ_y, and ε_u represents the ultimate strain. Under the above assumptions, the problem of the ultimate strength analysis of steel cross-sections can be formulated as:

Given a strain distribution corresponding to a failure condition, find the ultimate resistances N, M_x, M_y so as to fulfil the basic equations of equilibrium and the following linear constraints:

$$\begin{cases} L_1\left(N,M_x,M_y\right) \equiv M_x - M_{x0} = 0 \\ L_2\left(N,M_x,M_y\right) \equiv M_y - M_{y0} = 0 \end{cases} \quad (12a)$$

$$\begin{cases} L_1\left(N, M_x, M_y\right) \equiv N - N_0 = 0 \\ L_2\left(N, M_x, M_y\right) \equiv M_y - \tan(\alpha) M_x = 0 \end{cases} \tag{12b}$$

where N_0, Mx_0, M_{y0} represent the given axial force and bending moments.

Corresponding to the linear constraint (12) we can define a point on the failure surface as: (I) when the constraints (12a) are injected in the nonlinear system (11), a point on the failure surface is defined computing the axial resistance N associated with a failure criterion and for a fixed value of bending moments (M_{x0}, M_{y0}); (II) when constraints (12b) are used, the point on the failure surface is defined for a fixed axial load (N_0) and a given bending moment's ratio. The failure diagrams correspond to maximum strains attained at the outer compressed or tensioned point of the steel section (i.e. ε_u equal to the strain at failure). For each inclination of the neutral axis defined by the parameters ϕ_x and ϕ_y the farthest point on the compressed or tensioned side is determined (i.e. the point with co-ordinates x_c, y_c). Assuming that the failure condition is achieved in this point, the resulting strain distribution corresponding to the curvatures ϕ_x and ϕ_y can be expressed in linear form as in Eq.(2). Then, substituting the strain distribution given by the Eq. (2) in the basic equations of equilibrium, the unknown u together with the failure constraint equation can be eliminated from the nonlinear system (11). Thus, the nonlinear system of equations (11) is reduced to an only three basic equations of equilibrium and together with one of the linear constraints (Eq. 12), forms a determined nonlinear system of equations, and the solutions can be obtained iteratively following the procedure described in [6].

2.1.2 Macro model formulation

In this approach the gradual plastification of the cross section of each member are accounted for by smooth force-generalized strain curves, experimentally or numerically calibrated. In the present elasto-plastic frame analysis approach, gradual plastification through the cross-section subjected to combined action of axial force and biaxial bending moments may be described by moment-curvature-thrust (M-Φ-N), and moment-axial deformation-thrust (M-ε-N) curves that are calibrated by numerical tests. In order to take into account more explicitly the effect of residual stresses of the cross-sections we propose another smooth force-strain curve to model the gradual-plastification. The proposed relations modify the force-strain relations proposed by the Albermani [7] in order to simulate a nonlinear variation of the cross-section axial and flexural rigidity. The behaviour of a cross-section subjected to the combined action of axial force and bending moments is expressed in a set of equations relating the bending moments (axial forces) and the flexural (axial) rigidity for a certain value of axial force:

$$K_T = \begin{cases} K_0, & F < F_{yield} \\ K_0 \left[1 - \left(\dfrac{F - F_{yield}}{F_p - F_{yield}} \right)^{\alpha} (1-p) \right], & F_{yield} \le F \le F_p \\ pK_0, & F > F_p \end{cases} \quad (13)$$

where:

K_T - represents the tangent axial or flexural rigidity about either strong or weak flexural axis;

K_0 - represents the constant reference flexural/axial rigidity;

F - represents the cross-sectional generalized force (axial or bending moment with respect to either strong or weak cross-sectional axis);

F_{yield} - represents the generalized force (axial or bending moment) at first yield

F_p - represents the full plastification force;

p - represents a strain-hardening parameter, for p=0 the strain-hardening effect is neglected;

α - represents a shape parameter to express the nonlinear variations of the tangent flexural/axial rigidity of cross-section; for α=1 we find the Albermani equations.

The shape parameters p and α are determined throughout numerical calibrations. The effects of the combined action of axial force (N) and bi-axial bending moments (M_y, M_z) and as well the effect of residual stresses are taken into account in the expressions of the first yielding (F_{yield}) and full plastification (F_p) generalized forces. For instance, the full plastification bending moment is obtained from the full plastification surface equation for a given values of bending moments and axial force, whereas the first yielding bending moment is expressed as:

$$M_{yield,y(z)} = \left(\sigma_y - \sigma_r - \frac{N}{A} - \frac{M_{y(z)}}{W_{el,y(z)}} \right) W_{el,y(z)} \quad (14)$$

where σ_y represents the yield stress, σ_r represents the maximum value of residual stress, A the area of the cross-section, and W_{el} represents the elastic section modulus of the cross-section with respect to strong or weak flexural axes. For α=1, as is proposed by Albermani, a linear stiffness degradation is considered. However, for steel cross-sections, where the effects of residual stresses are significantly on the inelastic behavior, a nonlinear stiffness degradation is required to represents adequately the partial plastification effects associated with bending and axial forces. The effect of axial forces on the plastic moments capacity of sections is considered by standard strength interaction curves.

2.2 Flexibility based derivations. Member analysis

Flexibility-based method is used to formulate the distributed plasticity model of a 3D frame element (12 DOF) under the above assumptions. An element is represented by several cross sections (i.e. stations) that are located at the numerical

integration scheme points (Figure 2a). The spread of inelastic zones within an element is captured considering the variable section flexural EI_y and EI_z and axial EA rigidity along the member length, depending on the bending moments and axial force level, cross-sectional shape and nonlinear constitutive relationships as already described. Figure 2b shows the deformed shape of a 3D beam-column element in local system attached to the initially straight center line, with the rigid body modes removed. Non-linear analysis by the stiffness method requires incremental loading, i.e. the inelastic behaviour is approximated by a series of elastic analysis. The element incremental flexibility matrix $\mathbf{f}_r$ which relates the end displacements to the actions $\Delta\mathbf{s}_r$ can be derived directly from energetic principles. Assuming elastic behaviour within a load increment, and no coupling of axial and flexural responses at the section level, the increment of the strain energy ΔW can be written as follows, including the additional shear and torsional deformations, Fig. 2:

$$\Delta W = \frac{L}{2}\int_0^1 \frac{N^2}{EA(\xi)}d\xi + \frac{L}{2}\int_0^1 \frac{M_z^2(\xi)}{EI_z(\xi)}d\xi + \frac{L}{2}\int_0^1 \frac{M_y^2(\xi)}{EI_y(\xi)}d\xi + \frac{L}{2}\int_0^1 \frac{M_x^2}{GI_t(\xi)}d\xi + \frac{L}{2}\int_0^1 \frac{T_y^2(\xi)}{GA_y(\xi)} + \frac{L}{2}\int_0^1 \frac{T_z^2(\xi)}{GA_z(\xi)} \quad (15)$$

in which the bending moments and shear forces are given by the following equations, supposing that the element is subjected to uniform distributed loads $q_{y(z)}$:

$$\begin{aligned} M_{y(z)}(\xi) &= M_{iy(z)}(\xi - 1) + M_{jy(z)}\xi + \frac{q_{y(z)}L^2\xi(\xi-1)}{2} \\ T_{y(z)}(\xi) &= \frac{dM_{y(z)}(\xi)}{d\xi} = \frac{M_{iy(z)} + M_{jy(z)}}{L} + \frac{q_{y(z)}L^2(2\xi-1)}{2} \end{aligned} \quad (16)$$

Using the second theorem of Castigliano the relationship between incremental deformations and efforts can be readily calculated and partitioned as follows:

$$\begin{bmatrix} u \\ \theta_{iy} \\ \theta_{jy} \\ \theta_{iz} \\ \theta_{jz} \\ \theta_x \end{bmatrix} = \begin{bmatrix} \frac{\partial \Delta W}{\partial N} \\ \frac{\partial \Delta W}{\partial M_{iy}} \\ \frac{\partial \Delta W}{\partial M_{jy}} \\ \frac{\partial \Delta W}{\partial M_{iz}} \\ \frac{\partial \Delta W}{\partial M_{jz}} \\ \frac{\partial \Delta W}{\partial M_x} \end{bmatrix} = \begin{bmatrix} \mathbf{f}_{1(3x3)} & \mathbf{0}_{(3x3)} \\ \mathbf{0}_{(3x3)} & \mathbf{f}_{2(3x3)} \end{bmatrix} \cdot \begin{bmatrix} N \\ M_{iy} \\ M_{jy} \\ M_{iz} \\ M_{jz} \\ M_x \end{bmatrix} + \begin{bmatrix} 0 \\ \delta_{iy} \\ \delta_{jy} \\ \delta_{iz} \\ \delta_{jz} \\ 0 \end{bmatrix} \quad (17)$$

or in a condensed form:

$$\Delta\mathbf{u}_r = \mathbf{f}_r \cdot \Delta\mathbf{s}_r + \boldsymbol{\delta}_r \quad (18)$$

where $\mathbf{f}_r$ represents the incremental flexibility matrix of the beam-column element without rigid body modes, and in which the matrices $\mathbf{f}_i$ (i=1,2) have the following expressions:

$$\mathbf{f}_1 = \begin{bmatrix} L\int_0^1 \frac{1}{EA(\xi)}d\xi & 0 & 0 \\ 0 & L\int_0^1 \frac{(\xi-1)^2}{EI_y(\xi)}d\xi + \frac{1}{L}\int_0^1 \frac{d\xi}{GA_y(\xi)} & L\int_0^1 \frac{\xi(\xi-1)}{EI_y(\xi)}d\xi + \frac{1}{L}\int_0^1 \frac{d\xi}{GA_y(\xi)} \\ 0 & L\int_0^1 \frac{\xi(\xi-1)}{EI_y(\xi)}d\xi + \frac{1}{L}\int_0^1 \frac{d\xi}{GA_y(\xi)} & L\int_0^1 \frac{\xi^2}{EI_y(\xi)}d\xi + \frac{1}{L}\int_0^1 \frac{d\xi}{GA_y(\xi)} \end{bmatrix} \tag{19.a}$$

$$\mathbf{f}_2 = \begin{bmatrix} L\int_0^1 \frac{(\xi-1)^2}{EI_z(\xi)}d\xi + \frac{1}{L}\int_0^1 \frac{d\xi}{GA_z(\xi)} & L\int_0^1 \frac{(\xi-1)^2}{EI_z(\xi)}d\xi + \frac{1}{L}\int_0^1 \frac{d\xi}{GA_z(\xi)} & 0 \\ L\int_0^1 \frac{(\xi-1)^2}{EI_z(\xi)}d\xi + \frac{1}{L}\int_0^1 \frac{d\xi}{GA_z(\xi)} & L\int_0^1 \frac{(\xi-1)^2}{EI_z(\xi)}d\xi + \frac{1}{L}\int_0^1 \frac{d\xi}{GA_z(\xi)} & 0 \\ 0 & 0 & L\int_0^1 \frac{d\xi}{GI_t(\xi)} \end{bmatrix} \tag{19.b}$$

and $\boldsymbol{\delta}_r$ is a term resulting from loading actions. To produce the deformational-stiffness relation, the Equation (18) is inverted, resulting the following deformational-stiffness equation:

$$\Delta\mathbf{s}_r = \mathbf{k}_r \cdot \Delta\mathbf{u}_r - \mathbf{q}_r \tag{20}$$

where the vector $\mathbf{q}_r$ is the equivalent load vector, whereas $\mathbf{k}_r$ represents the instantaneous element stiffness matrix of the beam-column element without rigid body modes, determined by matrix inversion of the flexural matrix f_r:

$$\mathbf{k}_{r(6x6)} = \mathbf{f}_r^{-1} = \begin{bmatrix} \mathbf{f}_1^{-1} & \mathbf{0} \\ \mathbf{0} & \mathbf{f}_2^{-1} \end{bmatrix} = \begin{bmatrix} \mathbf{k}_{1(3x3)} & \mathbf{0}_{(3x3)} \\ \mathbf{0}_{(3x3)} & \mathbf{k}_{2(3x3)} \end{bmatrix} \tag{21}$$
$$\mathbf{q}_r = \mathbf{k}_r \boldsymbol{\delta}_r$$

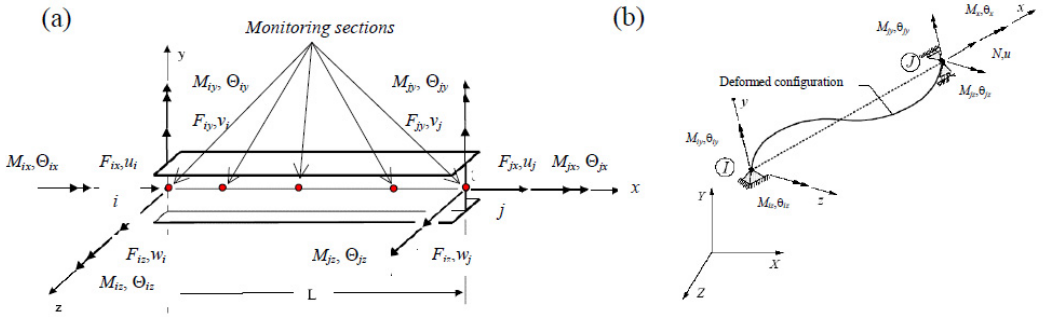

Figure 2: (a) Beam column element with 12 DOF; (b) Beam column element with rigid body modes removed.

The resulting element stiffness matrix is a 6x6 matrix. To include rigid body modes, the stiffness matrix is pre- and post multiplied by a transformation matrix to result in the required 12 x12 matrix.

2.2 The second order effects on element tangent stiffness matrix

The geometrical nonlinear effects for each element are taken into account in the present analysis, in a beam column approach, by the use of the inelastic stability stiffness functions and updating at each load increment the length, axial force and the flexural rigidity about of each principal axes of the element. This way minimizes modelling and solution time, generally only one or two elements are needed per member. The element force fields are described by the second order transfer matrix as function of the nodal element forces [5].

2.3 The effect of plastic surface on element tangent stiffness matrix

If the state of forces at any cross-section along the beam column element equals or exceeds the plastic section capacity, the flexural stiffness at the respective location approaches zero. Once the member forces get to the full plastic surface, and strain-hardening is neglected, they are assumed to move on the plastic surface at the following loading step (Fig.3). Therefore, when the axial force of a member increases at the following loading step, the incremental force-displacement relationships at the element level has to be modified such that the loading result in motion along the interaction surfaces and the plastic strength surface requirement of the full plastified sections is always satisfied. We assume the general case when limit surfaces are not linear; these surfaces can be regarded to be incrementally linear. In this way, for the fully plastified cross-sections, the relationship between incremental axial forces and bending moments can be linearized as well. Considering the member in Fig.2 and that at the end of the member at node *i* the forces (N, M_y, M_z) get to the full plastic surface the incremental bending moments ΔM_{iy} , ΔM_{iz} and the incremental axial force ΔN are linearly related as (Fig.3):

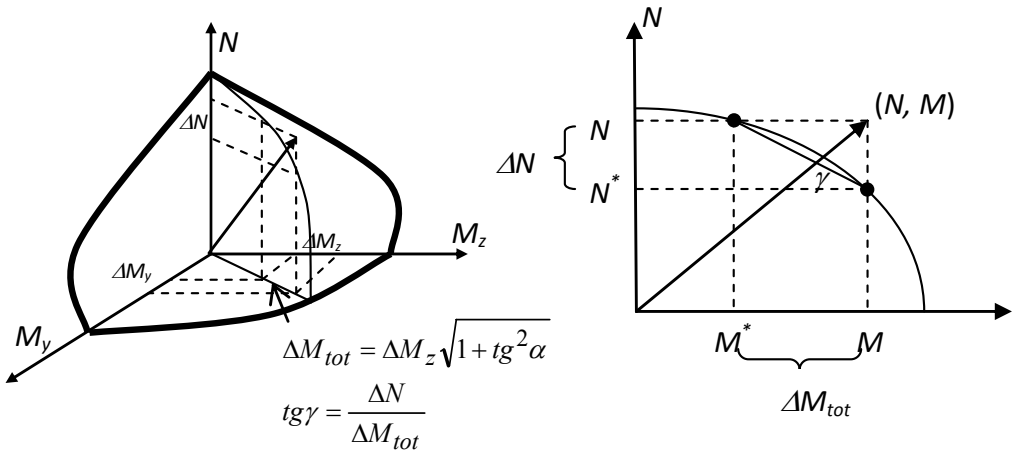

Figure 3: The effect of plastic surface on element tangent stiffness matrix.

$$\Delta M_{iz} = \frac{1}{tg\gamma\sqrt{1+tg^2\alpha}}\Delta N = c_z \Delta N$$
$$\Delta M_{iy} = \frac{tg\alpha}{tg\gamma\sqrt{1+tg^2\alpha}}\Delta N = c_y \Delta N \tag{22}$$

where:

$$\Delta M = M_{tot} - M^*$$
$$\Delta N = N - N^* \tag{23}$$

and in which M^* represents the ultimate total bending moment associated to given value of axial force N and N^* represents the ultimate axial force for given value of total bending moment $M_{tot} = M_z\sqrt{1+tg^2\alpha}$. When the fiber cross-section analysis is applied the ultimate efforts (M^* and N^*) are determined using the numerical procedure described at section 2.1.12. Consequently the basic nodal element forces for the beam column element can be expressed in matrix form as:

$$\begin{bmatrix} \Delta N \\ \Delta M_{iy} \\ \Delta M_{jy} \\ \Delta M_{iz} \\ \Delta M_{jz} \end{bmatrix} = \begin{bmatrix} 1 & 0 & 0 & 0 \\ c_y & 0 & 0 & 0 \\ 0 & 1 & 0 & 0 \\ c_z & 0 & 0 & 0 \\ 0 & 0 & 0 & 1 \end{bmatrix} \begin{bmatrix} \Delta N \\ \Delta M_{jy} \\ \Delta M_{iz} \\ \Delta M_{jz} \end{bmatrix} \tag{24}$$

or symbolically in condensed matrix form:

$$\Delta \mathbf{s}_{r(5x1)} = \mathbf{T}_{c(5x4)} \Delta \hat{\mathbf{s}}_{(4x1)} \tag{25}$$

where the transformation matrix $\mathbf{T}_c$ introduce the correlation between nodal forces such that the plastic strength surface requirement at section "*i*" is not violated by the change of member forces after the full plastic strength of cross-section is reached (Fig.3). Denoting $\Delta \mathbf{s}_r$, $\Delta \mathbf{u}$ and $\Delta \mathbf{q}_r$ as finite changes in the force vector, displacement vector and fixed-end force vector, respectively, the incremental force-displacement relationship for the element including the equivalent nodal loads can be expressed as:

$$\Delta \mathbf{s}_r = \mathbf{k}_r \Delta \mathbf{u} + \Delta \mathbf{q}_r \tag{26}$$

and which inverted gives:

$$\mathbf{f}_r \Delta \mathbf{s}_r = \Delta \mathbf{u} + \mathbf{f}_r \Delta \mathbf{q}_r \tag{27}$$

where $\mathbf{f}_r$ represents the flexibility matrix of the element. Both stiffness $\mathbf{k}_r$ and flexibility $\mathbf{f}_r = \mathbf{k}_r^{-1}$ matrices include the effects of material and geometrical nonlinear effects as described in above sections. We mention just that the rows and columns

associated to the torsional degree of freedom have been removed in the matrix representation in the equations (26) and (27).

Substituting Eq.(25) for $\Delta\mathbf{s}_r$ into Eq.(27) gives:

$$\mathbf{f}_r\mathbf{T}_c\Delta\hat{\mathbf{s}} = \Delta\mathbf{u} + \mathbf{f}_r\Delta\mathbf{q}_r \tag{28}$$

Multiply both members of Eq.(28) with $\mathbf{T}_c{}^T$ and solving for $\Delta\hat{\mathbf{s}}$ we obtain:

$$\Delta\hat{\mathbf{s}} = \left(\mathbf{T}_c{}^T\mathbf{f}_r\mathbf{T}_c\right)^{-1}\mathbf{T}_c{}^T\Delta\mathbf{u} + \left(\mathbf{T}_c{}^T\mathbf{f}_r\mathbf{T}_c\right)^{-1}\mathbf{T}_c{}^T\mathbf{f}_r\Delta\mathbf{q}_r \tag{29}$$

The equations (27) and (29) can now be combined by realizing that the basic force-displacement relationship is given by:

$$\Delta\mathbf{s}_r = \mathbf{T}_c\left(\mathbf{T}_c{}^T\mathbf{f}_r\mathbf{T}_c\right)^{-1}\mathbf{T}_c{}^T\Delta\mathbf{u} + \mathbf{T}_c\left(\mathbf{T}_c{}^T\mathbf{f}_r\mathbf{T}_c\right)^{-1}\mathbf{T}_c{}^T\mathbf{f}_r\Delta\mathbf{q}_r \tag{30}$$

or symbolically in condensed matrix form:

$$\Delta\mathbf{s}_r = \mathbf{k}_{r,ep}\Delta\mathbf{u} + \Delta\mathbf{q}_{rp} \tag{31}$$

where $\mathbf{k}_{r,ep}$ and $\Delta\mathbf{q}_{rp}$ represents the stiffness matrix and equivalent nodal loads vector for the element when a full plastified cross section forms at the *i*-th end of the element:

$$\mathbf{k}_{r,ep} = \mathbf{T}_c\left(\mathbf{T}_c{}^T\mathbf{f}_r\mathbf{T}_c\right)^{-1}\mathbf{T}_c{}^T \tag{32}$$

$$\Delta\mathbf{q}_{rp} = \mathbf{T}_c\left(\mathbf{T}_c{}^T\mathbf{f}_r\mathbf{T}_c\right)^{-1}\mathbf{T}_c{}^T\mathbf{f}_r\Delta\mathbf{q}_r \tag{33}$$

Following a similar approach we can obtain the elasto-plastic stiffness matrix and equivalent nodal loads for the cases when a full plastified sections forms at *j*-th end of the member or at both ends.

2.4 The effects of joint flexibility

The behaviour of the connection element in each principal bending direction (major and minor axis flexibility) is represented by a rotational dimensionless spring attached to the member ends (Figure 4). We assume no coupling between different rotational degree of freedom at the connection. The present formulation can model both major and minor axis flexibility.

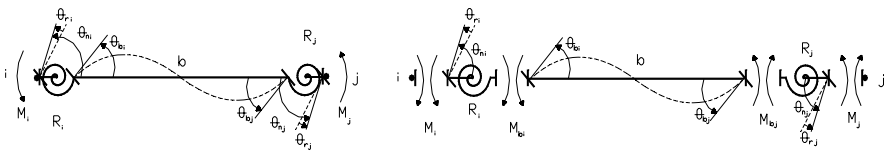

Figure 4: Beam-column element with semi-rigid connections.

The effects of semi-rigid connections are included in the analysis adopting the mathematical model developed in [5]. The stiffness matrix and equivalent nodal loads vector, considering the effects of flexible connections can be determined as:

$$\begin{aligned} \mathbf{k}_{sem(4x4)} &= \mathbf{k}_{r(4x4)} - \mathbf{k}_{r(4x4)}\left(\mathbf{k}_{r(4x4)} + \mathbf{k}_{sc(4x4)}\right)^{-1}\mathbf{k}_{r(4x4)} \\ \Delta\mathbf{q}_{sem(4x1)} &= \Delta\mathbf{q}_{eq(4x1)} - \Delta\mathbf{q}_{eq(4x1)}\mathbf{k}_{r(4x4)}\left(\mathbf{k}_{r(4x4)} + \mathbf{k}_{sc(4x4)}\right)^{-1} \end{aligned} \tag{34}$$

where $\mathbf{k}_r$ represents the stiffness matrix of the rigid ended element including the effects of material and geometrical nonlinearities, $\Delta\mathbf{q}_{eq}$ represents the equivalent nodal loads for rigid ended element, $\mathbf{k}_{sc}$ represents the stiffness matrix of the semi-rigid connections that can be expressed as $\mathbf{k}_{sc} = diag(R_{iy}, R_{jy}, R_{iz}, R_{jz})$ in which R_i, R_j are the instantaneous connection stiffness about both major (z) and minor (y) axis flexibility. If the connection behaviour is nonlinear, the connection model adopted in accordance with experimental model proposed in [8] can be used.

2.5 Geometry updating and analysis algorithm

In order to trace the equilibrium path, for proportionally and non-proportionally applied loads, the proposed model has been implemented in a simple incremental and incremental- iterative matrix structural-analysis program. In the simple incremental method, the simple Euler stepping algorithm is used in conjunction with constant work-load increments. In the incremental-iterative approach, at each load increment a modified constant arc-length method is applied to compute the complete nonlinear load-deformation path. Using an updated Lagrangian formulation (UL) the nonlinear geometrical effects are considered updating the element forces and geometry configurations at each load increment. The natural deformation approach (NDA) in conjunction with the geometrical "rigid body qualified" stiffness matrix [9] is adopted for the element force recovery and the web plane vector approach is effectively used to update the frame element coordinates [5].

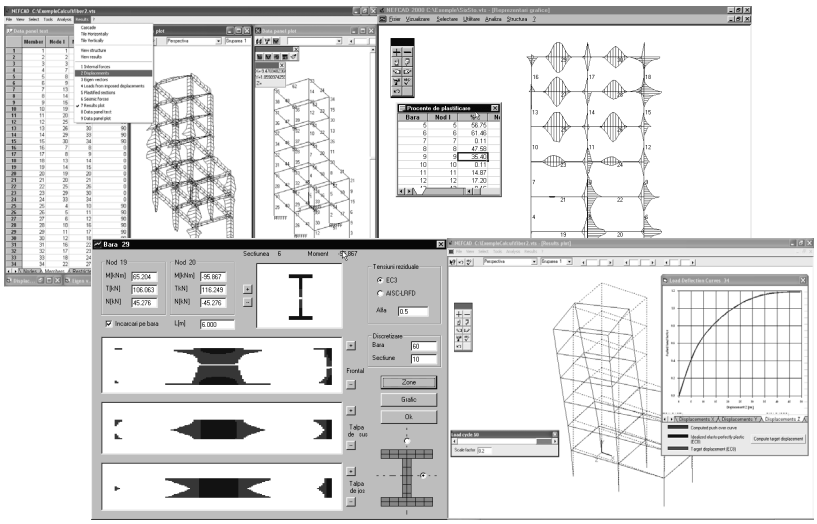

Figure 5: *NEFCAD* screen-shots.

3 Computer program description

Based on the analysis algorithm just described, an object-oriented computer program, *NEFCAD*, has been developed to study the combined effects of material, geometric and semi-rigid connection nonlinear behaviour on the load-versus-deflection response for spatial framed structures. It combines the structural analysis routine with a graphic routine to display the final results (Figure 4). The computational engine was written in Compaq Visual Fortran. The graphic interface was created using Microsoft Visual Basic 6. Dynamic Link Libraries (DLL) are used to communicate between the interface and engine. The computer program includes modules that provide for several kinds of analyses: linear static and eigen analysis; advanced nonlinear inelastic analysis. All these modules feature powerful and completely integrated design modules for steel frameworks, available from within the same interface used to create and analyze the model.

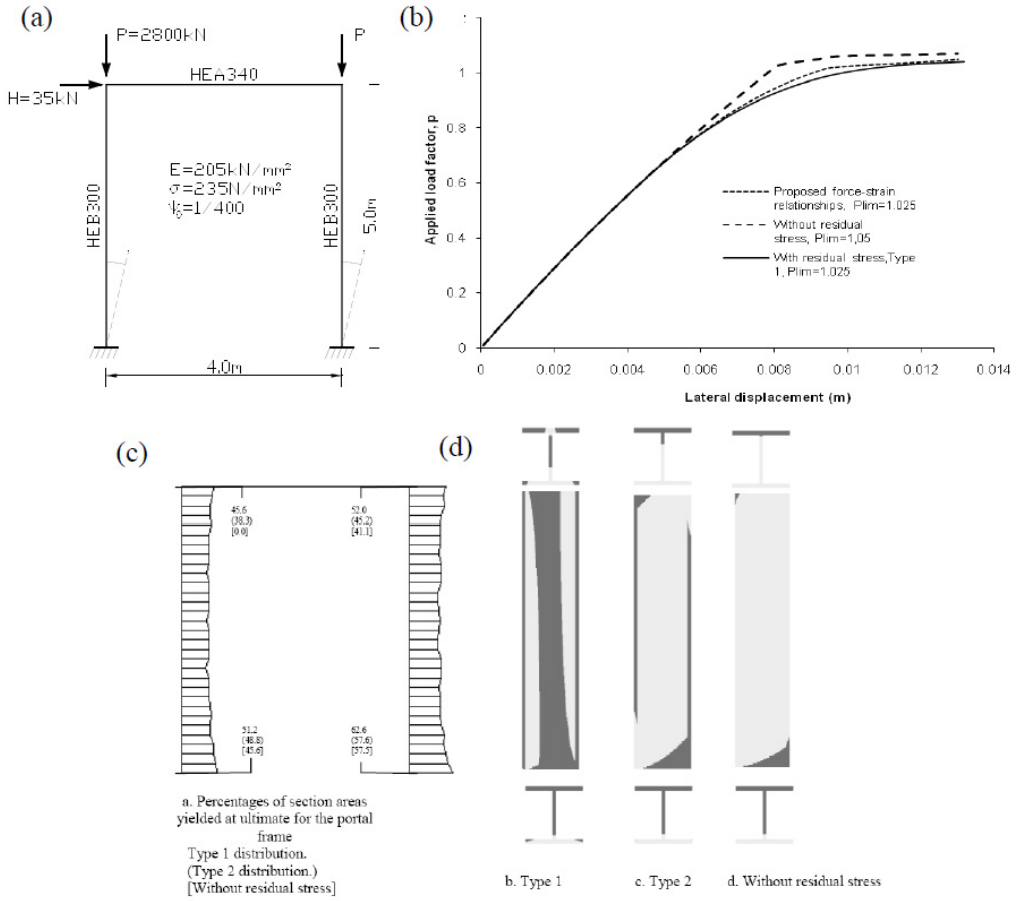

Figure 6: (a) Portal frame description; (b) Lateral load-displacement curves; (c) Percentages of section area yielded; (d) Spread of plastic zones.

4 Computational examples

4.1 Example 1: Portal frame

The portal frame in Figure 6a, which was first analysed by Vogel [10], has been considered one of the most sensitive to spreading of plasticity effects. The frame was analysed using the proposed model in two different ways. Firstly, the elasto-plastic behaviour is modelled accounting for spread-of-plasticity and residual stress effects in sections and along the member length through basic equilibrium, compatibility and material nonlinear constitutive equations σ-ε, in any section by an iterative process (e.g. micro model approach). Ramberg-Osgood stress-strain relationships with shape parameter n=30 and two residual stress patterns (EC3-Type 1 and AISC-LRFD-Type 2) have been considered. Secondly, in each section, the proposed analytical force-strain relationships are used computing the variable flexural EI and axial EA rigidity. The plastic zone developments are represented in the Figures 6c and 6d. Percentages of section-areas yielded and spread of plastic zones in the characteristic cross-sections are represented. In Figure 6b the comparable lateral-load displacement curves are represented for both models. As it can be seen, using the proposed force-strain analytical curve (α=2, p=0.001) the elasto-plastic behaviour can be calibrated to model the explicit plastic zone analysis.

4.2 Example 2: Six story steel space frame

The Orbison's six story rigid space frame (Figure 7a), studied previously by other researchers [1, 2] was used in the verification study. The effects of rigid and semi-rigid connections, with either linear or nonlinear behaviour, of the space frame has been investigated. In the case of semi-rigid beam-columns connections, the beam connections were top and seat angles having the following characteristics: (1) at the beam framing about the major-axis of column the fixity factor g=0.86, ultimate moment M_u=300kNm, shape parameter n=1.57, (2) at the beam framing about the minor-axis of column, the fixity factor g=0.86, ultimate moment M_u=200 kNm, shape parameter n=0.86 [8]. The yield strength of all members is 250 MPa, Young´s modulus is E=206850 MPa and shear modulus G=79293 MPa. The frame is subjected to the combined action of gravity and lateral loads acting in the Y-direction. Uniform floor pressure is 9.6 kN/m^2 and the wind loads are simulated by point loads of 53.376 kN in the Y direction at every beam-column joints. One element with seven integration points (NG=7) has been used to model each column and beam; gradual plastification through the cross-section is modelled using the proposed inelastic force strain relationships with the shape parameters α=2 and p=0.001 and by explicit integration of stresses and strains over the cross-section using Ramberg-Osgood stress-strain relationships with shape parameter n=30. Residual stress patterns according to EC3 have been considered. Comparing the nonlinear response obtained by the proposed approach with the explicit fiber-element approach of Jiang et.al. [2] an excellent agreement can be observed (Figure 8). However the proposed analysis implies only one element per physical member

whereas Jiang's method require nine elements per member in frame modelling to achieve the same accuracy and convergence.

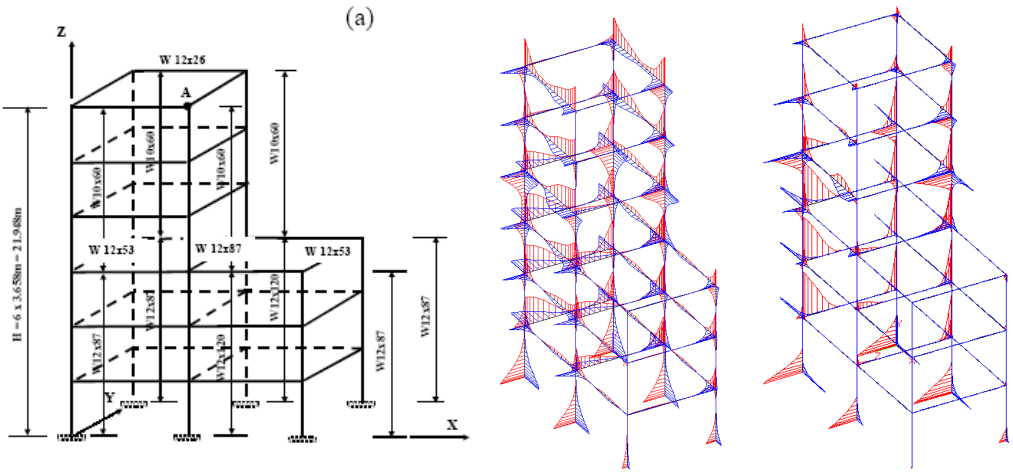

Figure 7: Six-story steel space frame: (a) Perspective view; (b) Flexural rigidities distribution-*micro model formulation* (c) Flexural rigidities distribution-*macro model formulation*;

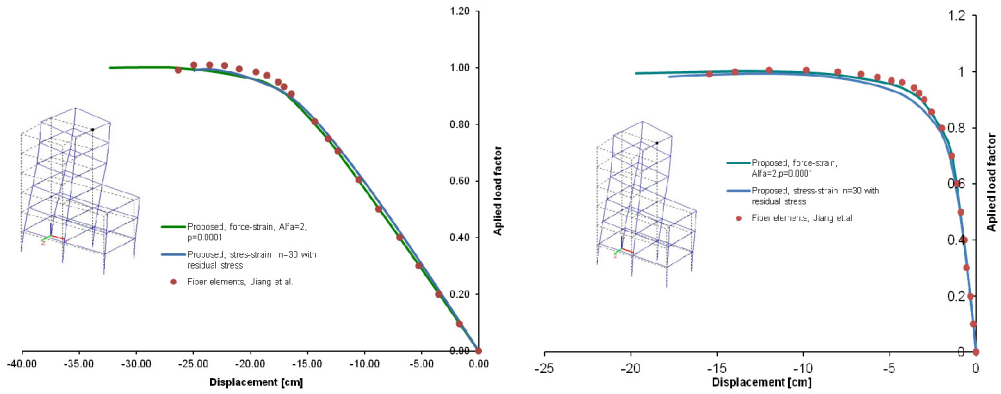

Figure 8: (a) Load-displacement curves at Y-dirrection of node A; (b) load-displacement curves at X dirrection of node A.

Figure 7 b, c shows the distribution of the flexural rigidities ($1\text{-}EI_t/EI_0$) along the member lengths at the ultimate load factor in the case of modelling the elasto-plastic behaviour at fibre level (micro model formulation) and at section level (macro model formaulation) respectivelly. The load displacement curves of rigid and semi-rigid connections (with linear or nonlinear behaviour), are compared in Figure 9. As it can be seen, semi-rigid connection is a very crucial element, and must be considered in a valuable advanced analysis method. This frame, subjected to three ground motions is considered further as a case study for seismic performance assessment. Three levels of ground motions, with the intention of checking different performance objectives have been considered. Ground motion is defined with the

Type I for elastic response spectrum and ground type *A* was assumed in analysis and a 5% damped response spectrum for every peak ground acceleration is assumed (Eurocode 8).

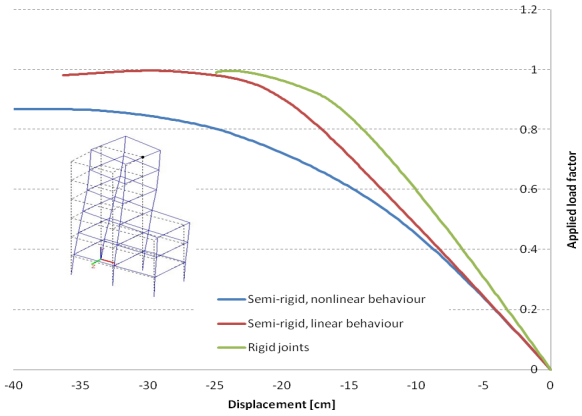

Figure 9: Load-displacement curves at *Y*-dirrection of node *A*: influence of semi-rigid connections.

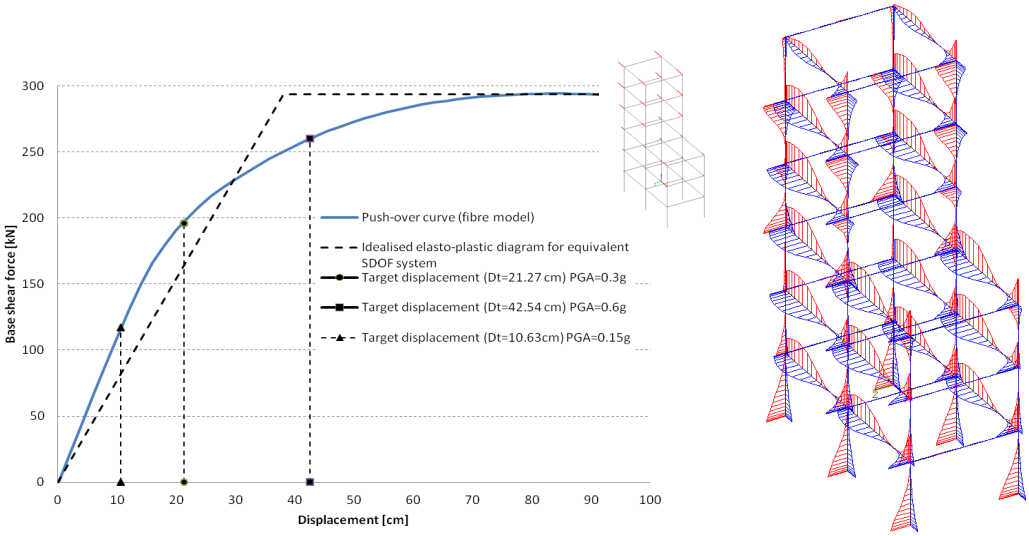

Figure 10: (a) Push-over curve and target displacements; (b) distribution of flexural rigidities at collapse.

The frame is subjected to the non-proportional action of gravity loads and lateral seismic loads. Uniform floor pressure is 9.6 kN/m^2 and represents the first sequence of loading. The seismic loads are simulated by point loads in the *X* direction at every beam-column joints using the 3D modal load pattern corresponding to first mode in longitudinal direction (Fig. 10a). The nonlinear analysis of this frame was conducted using the proposed explicit fiber beam-column element. The pushover curve of control node *A* at the top of the frame is shown in Figure 10. In order to compute the displacement demands, idealize the pushover curve as a bilinear elasto-perfectly plastic force displacement relationship represent the next step of pushover analysis.

Pushover curves and the corresponding SDOF capacity diagram for longitudinal direction is depicted in Figure 10a. Also the corresponding target displacements for three earthquake intensities PGA = 0.15 g, PGA = 0.30 g and 0.6 g are placed on the MDOF pushover curve. Figure 10b shows the variation of the flexural rigidities ($1-EI_t/EI_0$) along the member lengths at collapse. Running on a laptop computer with 2GHz processor, the proposed fiber analysis was performed in approximately 3 minutes.

5 Conclusions

A reliable and robust nonlinear inelastic analysis method for semi-rigid space frames has been developed. The proposed model is based on the most refined type of second order inelastic analysis, the plastic zone analysis. The proposed analysis can practically account for all key factors influencing steel space frame behaviour: gradual and distributed yielding associated with biaxial bending and axial force, shear deformations, local and global second order effects, and nonlinear behaviour of semi-rigid connections, with computational efficiency, and the necessary degree of accuracy, usually only one element per member is necessary to analyse. Furthermore, distributed loads acting along the member length can be directly input into the analysis without the need to divide a member into several elements. The model has been implemented in an incremental-iterative matrix structural analysis program and allows proportionally and non-proportionally loading, and has been verified by comparing the predicted results with the established results available from the literature. The studies show that the proposed analysis compares very well to finite fibre element solution with much less computational effort. The proposed software is presented as an efficient, reliable tool ready to be implemented into design practice for advanced analysis and pushover analysis of spatial frame structures. However, a fundamental assumption made for pushover analysis is that first mode dominates, and that the higher mode effects are not significant. Future work is envisaged considering the effect the time variant distribution of inertial forces experienced by the structure.

Acknowledgment

The authors are thankful to the financial support by Romanian National Authority for Scientific Research (ANCS and CNCSIS) under the Grant PNII-IDEI No. 193/2008.

References

[1] Ngo-Huu C., Kim S.E., Oh,J.R., Nonlinear analysis of steel frames using fiber plastic hinge concept, Engineering Structures, 29(4): 649-657, 2007.

[2] Jiang, X.M, Chen, H. and Liew, JYR, Spread of plasticity analysis of three-dimensional steel frames, Journal of Constructional Steel Research, 58, 193-212, 2002.
[3] Antoniou, S. & Pinho, R., Development and verification of a displacement-based adaptive pushover procedures, Journal of Earthquake Engineering, 8(5): 643–661, 2004.
[4] Fajfar, P. & Gaspersic, P., The N2 method for the seismic damage analysis of RC buildings, Earthquake Engineering and Structural Dynamics, 25: 31–46, 1996.
[5] Chiorean C.G., A computer method for nonlinear inelastic analysis of 3D semirigid steel frameworks, Engineering Structures, 31(12): 3016–3033, 2009.
[6] Chiorean, C.G., Computerised interaction diagrams and moment capacity contours for composite steel-concrete cross-sections, Engineering Structures, 32(11): 3734–3757, 2010.
[7] Al-Bermani, F.G.A.and Zhu, K., Nonlinear elasto-plastic analysis of spatial structures under dynamic loading using kinematic hardening models, Engineering Structures, 18(8), 568-576, 1996.
[8] Chen, W.F. and Kishi, N., Semi-rigid steel beam-to-column connections, data base and modeling, Journal of Structural Engineering, ASCE, 115(1), 105-119, 1989.
[9] Yang, Y.B., Yau, J.D., Leu, L.J., Recent developments in geometrically nonlinear and postbuckling analysis of framed structures, Applied Mechanical Review, 56(4), 431-49, 2003.
[10] Vogel, U., Calibration frames, Sthalbau, 10, 1-7, 1985.